

³⁹Ar-⁴⁰Ar dating of the Zagami Martian shergottite and implications for magma origin of excess ⁴⁰Ar

Donald D. BOGARD* and Jisun PARK

ARES, Code KR, NASA Johnson Space Center, Houston, Texas 77058, USA

*Corresponding author. E-mail: donald.d.bogard@nasa.gov

(Received 17 September 2007; revision accepted 27 November 2007)

Abstract—The Zagami shergottite experienced a complex, petrogenetic formation history (McCoy et al. 1992, 1999). Like several shergottites, Zagami contains excess ⁴⁰Ar relative to its formation age. To understand the origin of this excess ⁴⁰Ar, we made ³⁹Ar-⁴⁰Ar analyses on plagioclase and pyroxene minerals from two phases representing different stages in the magma evolution. Surprisingly, all these separates show similar concentrations of excess ⁴⁰Ar, $\sim 1 \times 10^{-6}$ cm³/g. We present arguments against this excess ⁴⁰Ar having been introduced from the Martian atmosphere as impact glass. We also present evidence against excess ⁴⁰Ar being a partially degassed residue from a basalt that actually formed ~ 4 Gyr ago. We utilize our experimental data on Ar diffusion in Zagami and evidence that it was shock-heated to only ~ 70 °C, and we assume this heating occurred during an ejection from Mars ~ 3 Myr ago. With these constraints, thermal considerations necessitates either that its ejected mass was impossibly large, or that its shock-heating temperature was an order of magnitude higher than that measured. We suggest that this excess ⁴⁰Ar was inherited from the Zagami magma, and that it was introduced into the magma either by degassing of a larger volume of material or by early assimilation of old, K-rich crustal material. Similar concentrations of excess ⁴⁰Ar in the analyzed separates imply that this magma maintained a relatively constant ⁴⁰Ar concentration throughout its crystallization. This likely occurred through volatile degassing as the magma rose toward the surface and lithostatic pressure was released. These concepts have implications for excess ⁴⁰Ar in other shergottites.

INTRODUCTION

The formational history of the Zagami basaltic shergottite was complex, involving crystal cumulates, residual melts, flow differentiation, and melt migration, as was discussed in a series of papers by McCoy and co-workers (McCoy et al. 1992, 1995, 1999; and references therein). Zagami formed in a two-stage magmatic history, involving different depths and cooling histories (McCoy et al. 1992). The early formation of homogeneous, Mg-rich pyroxene cores implies slow cooling in a deep (>7 km) magma chamber. These were entrained in rising magma, partially corroded, and later were overgrown by Fe-rich rims. Pigeonite rims on augite cores suggest an interruption of pyroxene crystallization. Location of amphibole-bearing melt inclusions exclusively within pyroxene cores implies high-pressure crystallization of the cores and low-pressure crystallization of the Fe-rich rims (McCoy et al. 1992). Late in the crystallization sequence, pockets of magma formed mesostasis, plagioclase, and minor phases enriched in incompatible elements.

The more evolved portions of Zagami show variable pigeonite compositions, FeO-rich pyroxene clumps, and

enrichment in modal abundance of olivine. The Zagami meteorite displays areas, with distinct boundaries, whose texture is either coarse-grained (CG) or fine-grained (FG). These represent different stages in the magma composition and crystallization sequence, but in the hand specimen their relationship with the evolution sequence cannot always be discerned. Nyquist et al. (2006a) measured ⁸⁷Rb-⁸⁷Sr mineral isochrons for the CG and FG portions of Zagami and found them to have the same slopes (ages), but different ⁸⁷Sr/⁸⁶Sr initials (intercepts). This is additional evidence that these Zagami phases represent different magma compositions, which had insufficient time for Sr to equilibrate. Nyquist et al. (2006a) postulated that one component was derived from assimilation of a crustal component into the evolving magma. Further, several studies have suggested that the Shergotty basaltic shergottite, which is similar to Zagami, also experienced an analogous multi-stage formational history, with crystallization beginning at the 5–7 km depth, and the magma and mineral compositions evolving as the magma rose toward the surface (McCoy et al. 1995; Lentz and McSween 2000; McSween et al. 2001).

The crystallization age of Zagami has been determined

by the Sm-Nd, U-Pb, and Rb-Sr isotopic chronometers (Nyquist et al. [2001] and references therein; Borg et al. 2005; Bouvier et al. 2005). Although reported ages vary somewhat, especially the U-Pb ages, most workers prefer an age around 170 Myr, approximately the same as that of Shergotty and some other shergottites (Nyquist et al. 2001). We adopt a Zagami formation age of 170 Myr. However, the ^{39}Ar - ^{40}Ar age for Zagami, like most shergottites, is older than radiometric ages determined by other techniques. In some cases, these Ar-Ar ages were purposely measured on highly shocked shergottites or impact-produced glass veins and pockets, and the older ages have been attributed to the presence of shock-implanted Ar from the Martian atmosphere (Bogard and Johnson 1983; Bogard and Garrison 1999; Marti et al. 1995; Walton et al. 2007). However, this explanation is unlikely for some other shergottite phases with high Ar-Ar ages, and excess ^{40}Ar in some shergottites may be radiogenic ^{40}Ar inherited from the magma (Bogard and Garrison 1999; Bogard and Park 2007a; Walton et al. 2007).

A direct approach to test the idea that some excess ^{40}Ar ($^{40}\text{Ar}_{\text{xs}}$) in shergottites derived from the magma is to examine the concentrations of $^{40}\text{Ar}_{\text{xs}}$ in mineral separates of both the CG and FG portions of Zagami. We might expect $^{40}\text{Ar}_{\text{xs}}$ concentrations in Zagami to vary between CG and FG phases because of sampling at different stages in an evolving magma composition, and between pyroxene and plagioclase minerals because of crystallization at different times and/or degree of crystallization during magma evolution. For this purpose, we made ^{39}Ar - ^{40}Ar analyses of pyroxene and plagioclase (maskelynite) separates from both CG and FG Zagami. The Ar-Ar technique identifies ^{40}Ar from in situ decay relative to the formation age, if independently known, and thus, also $^{40}\text{Ar}_{\text{xs}}$. In this work we demonstrate that excess ^{40}Ar in Zagami represents neither shock-implanted Martian atmosphere nor undegassed ^{40}Ar from in situ decay in a rock that formed much earlier than 170 Myr ago. Rather, we argue that excess ^{40}Ar in Zagami was inherited from its magma and likely traces some aspects of the genesis and evolution of that magma. The results and conclusions arising from this experiment are relevant to understanding old apparent Ar-Ar ages of other Martian shergottites.

SAMPLES AND EXPERIMENTAL

We analyzed the same CG and FG samples of Zagami used by Nyquist et al. (2006a) for their studies. Mineral separation was performed by C.-Y. Shih at JSC using standard techniques. The samples were crushed to 100–200 mesh. Plagioclase was separated by magnetic susceptibility, and pyroxenes were separated by density using heavy liquids. Two different pyroxenes, labeled 1 and 2, with different magnetic susceptibilities were obtained from each sample. We refer to these separates as Px1 and Px2. We analyzed both Px1 and Px2 from the FG portion, but only Px2 from the CG

portion. Insufficient sample was available to analyze CG-Px1. We also analyzed the plagioclase separate from both CG and FG portions. As described below, these plagioclase separates also contained a mesostasis component. Although shock has transformed plagioclase feldspar to a different structural state, maskelynite or diaplectic glass, we will refer to these separates as CG-Plag and FG-Plag. Ar-Ar dating results for the CG-Plag were reported by Bogard and Garrison (1999). Results of the other analyses are reported here in Appendix 1.

The Zagami samples, along with other meteorites and 10 samples of the NL-25 hornblende age monitor, were neutron-irradiated at the University of Missouri reactor. The irradiation constant (J-value) differed slightly among samples, and had an average value of 0.0216. Argon was released by stepwise temperature extraction in a deep-well, ultra-high vacuum furnace equipped with a thermocouple, and its isotopic composition was measured on a VG-3600 mass spectrometer. Isotopic data were corrected for mass discrimination, system blanks, and reactor interferences. Additional experimental details are given in Bogard et al. (1995, 2000).

Ar-Ar RESULTS

Plagioclase

The Ar-Ar age spectra for plagioclase separates of Zagami CG and FG phases are shown in Fig. 1. Both samples show apparent Ar ages throughout the extractions that are higher than the preferred Zagami formation age of ~170 Myr, as determined by Sm-Nd and Rb-Sr isochrons (Nyquist et al. 2001; Borg et al. 2005). The K/Ca ratios decrease by more than an order of magnitude, from ~0.8 to values of 0.01–0.03 at the highest extraction temperatures. Electron probe studies of Zagami (Mikouchi et al. 1999; Mikouchi, personal communication, 2007) indicate that plagioclase (maskelynite) has variable K/Ca ratios of ~0.02–0.06, similar to the ratios in our plagioclase samples for about the last half of the ^{39}Ar release. Zagami also contains a K-rich mesostasis with variable K/Ca up to values as high as ~10. We attribute the first half of the ^{39}Ar release in our samples to a mixture of a few percent of this mesostasis and plagioclase, with the mesostasis contribution rapidly decreasing with increasing temperature. (Figure 1 shows K/Ca ratios for the FG sample, but ratios for the CG sample are similar.) That portion of the ^{40}Ar in these samples in excess of that which would form in situ over the past ~170 Myr is an excess component, $^{40}\text{Ar}_{\text{xs}}$. Similar ^{40}Ar excesses are observed in some other shergottites (e.g., Terribilini et al. 1998; Bogard and Garrison 1999; Walton et al. 2007).

To characterize the nature of $^{40}\text{Ar}_{\text{xs}}$ in these Zagami samples, we examined isochron plots of $^{40}\text{Ar}/^{36}\text{Ar}$ versus $^{39}\text{Ar}/^{36}\text{Ar}$. In principle, an isochron plot can distinguish $^{40}\text{Ar}_{\text{xs}}$ that is distributed through the lattice, such as ^{40}Ar inherited from the magma or ^{40}Ar from in situ

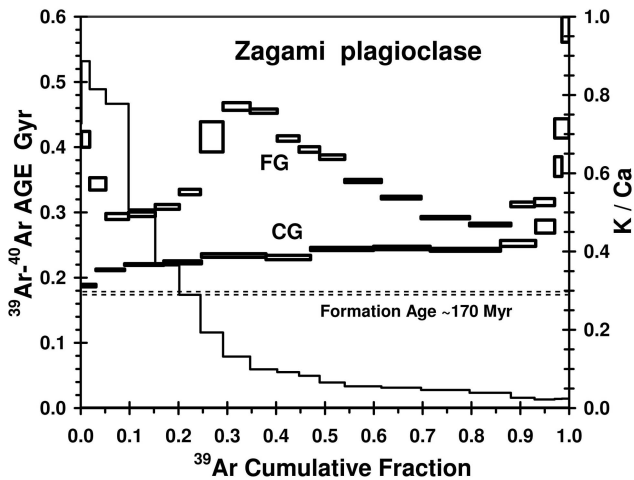


Fig. 1. ^{39}Ar - ^{40}Ar ages (rectangles, left axis) plotted against cumulative ^{39}Ar release for stepwise temperature extractions of plagioclase separates from coarse-grained (CG) and fine-grained (FG) Zagami phases. K/Ca ratios (stepped line, right axis) for the FG analysis are shown. The preferred Zagami formation age is also indicated.

decay that was incompletely degassed by a thermal event, from $^{40}\text{Ar}_{\text{xs}}$ added heterogeneously to the mineral, such as Martian or terrestrial ^{40}Ar introduced as shock-glass or arising from grain surface alteration. In considering such isochrons, it is desirable to utilize only one component of ^{36}Ar , either trapped or cosmogenic, as multiple ^{36}Ar components can produce isochron scattering. In much of these data, cosmogenic ^{36}Ar occurs in greater abundance than trapped ^{36}Ar . Thus, we usually normalize ^{40}Ar and ^{39}Ar to $^{36}\text{Ar}_{\text{cos}}$, whose concentration can be more accurately determined. We use the measured $^{36}\text{Ar}/^{37}\text{Ar}$ ratio to distinguish between these two ^{36}Ar components for each extraction (Garrison et al. 2000). In plagioclase, cosmogenic ^{36}Ar and ^{37}Ar are both nuclear components produced from Ca and are expected to have a constant ratio. Argon-37 is produced in the reactor, and $^{36}\text{Ar}_{\text{cos}}$ is produced in space by cosmic rays. The fact that the $^{39}\text{Ar}/^{36}\text{Ar}_{\text{cos}}$ and $^{40}\text{Ar}/^{36}\text{Ar}_{\text{cos}}$ ratios are observed to vary among extractions occurs because the K/Ca ratio decreases by more than an order of magnitude in both samples as the extraction proceeded (Fig. 1). We also examined isochron plots of $^{40}\text{Ar}/^{37}\text{Ar}$ versus $^{39}\text{Ar}/^{37}\text{Ar}$. Two advantages in normalizing to ^{37}Ar are that it is a single component and the $^{40}\text{Ar}/^{37}\text{Ar}$ and $^{39}\text{Ar}/^{37}\text{Ar}$ ratios have smaller measurement errors. The use of $^{36}\text{Ar}_{\text{cos}}$ and ^{37}Ar to normalize generally give very similar isochron results.

The isochron for CG plagioclase shown in Fig. 2 has been constructed using ^{37}Ar . CG-Plag gave nearly constant $^{36}\text{Ar}/^{37}\text{Ar}$ ratios for all extractions, which is indicative of a nearly pure nuclear component (i.e., no trapped ^{36}Ar was present). Using the minimum measured $^{36}\text{Ar}/^{37}\text{Ar}$ ratio, the total calculated cosmogenic ^{36}Ar in this CG plagioclase is $1.9 \times 10^{-9} \text{ cm}^3/\text{g}$, which is similar to previous determinations of $^{36}\text{Ar}_{\text{cos}}$ in Zagami and Shergotty (Eugster et al. 1997; Terribilini et al. 1998; Park 2005; Park et al. 2003; Schwenzer

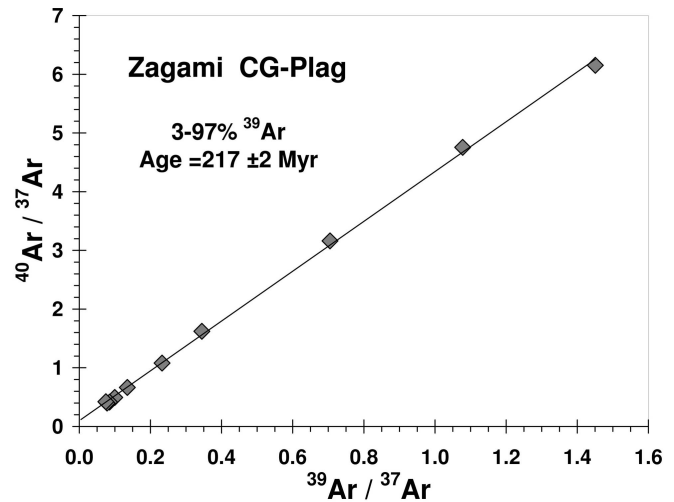


Fig. 2. Isochron plot of $^{40}\text{Ar}/^{37}\text{Ar}$ versus $^{39}\text{Ar}/^{37}\text{Ar}$ for 3–97% of the ^{39}Ar release for CG plagioclase. The first extraction released terrestrial atmospheric Ar, and the last extraction, showing the highest age, plots above the isochron; these data are not shown.

et al. 2007). The isochron age, calculated by weighing individual ratios by their individual uncertainties (Williamson 1968), is 217 ± 2 Myr. The isochron constructed by normalizing to $^{36}\text{Ar}_{\text{cos}}$, gives an age of 223 ± 21 Myr if we weigh ratios by their uncertainties and an age of 212 ± 2 Myr if we do not weigh the ratios. If we construct the isochron using total ^{36}Ar rather than $^{36}\text{Ar}_{\text{cos}}$, the age is 209 Myr. All of these isochron ages exceed the Sm-Nd and Rb-Sr mineral isochron ages for Zagami of 163–178 Myr (Borg et al. 2005; Nyquist et al. 2001).

The isochron plot for FG plagioclase normalized to $^{36}\text{Ar}_{\text{cos}}$ (Fig. 3) is more complex. The higher apparent Ar ages over much of the FG age spectrum compared to the CG spectrum (Fig. 1) indicate larger concentrations of $^{40}\text{Ar}_{\text{xs}}$ in FG-Plag, particularly at intermediate extraction temperatures. For the first half of the ^{39}Ar release, the $^{36}\text{Ar}/^{37}\text{Ar}$ ratios show a substantial decrease with increasing extraction temperature and indicate the release of a significant amount of trapped ^{36}Ar . However, the $^{36}\text{Ar}/^{37}\text{Ar}$ ratios are relatively constant for the last half of the ^{39}Ar release, indicating that ^{36}Ar was mostly cosmogenic. Thus, we adopted the lowest measured $^{36}\text{Ar}/^{37}\text{Ar}$ to calculate the $^{36}\text{Ar}_{\text{cos}}$ concentrations for each extraction. This gives a total $^{36}\text{Ar}_{\text{cos}}$ concentration for FG-Plag of $2.0 \times 10^{-9} \text{ cm}^3/\text{g}$, essentially identical to that obtained for CG-Plag. We constructed an isochron for these high temperature extractions using $^{36}\text{Ar}_{\text{cos}}$. Because trapped ^{36}Ar dominates over $^{36}\text{Ar}_{\text{cos}}$ for the first 50% of the ^{39}Ar release, we constructed isochrons for these extractions using trapped ^{36}Ar . The resulting FG isochron plot (Fig. 3) shows an unusual characteristic. All the data except those extractions showing a “hump” in apparent Ar age (25–54% ^{39}Ar release) define a reasonably linear trend. Those six extractions releasing 25–54% of the ^{39}Ar seem to define a parallel isochron with similar slope and defined Ar-Ar age (discussed

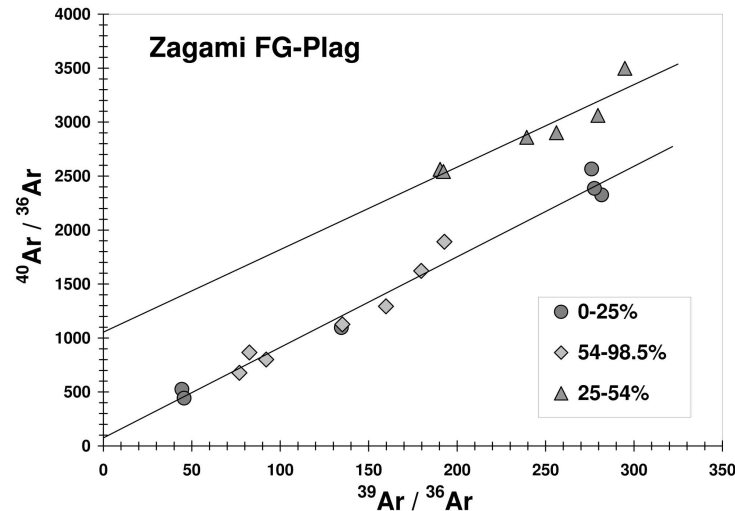


Fig. 3. Argon isochron plot for FG plagioclase. Extractions releasing 0–25% and 54–98.5% of the ^{39}Ar have been normalized to cosmogenic ^{36}Ar and define a single isochron. Extractions releasing 25–54% of the ^{39}Ar have been normalized to trapped ^{36}Ar and define a separate isochron. The two isochrons have the same slope but different intercepts. The two data points plotting highest above the lower isochron represent adjacent extractions to the component defining the upper isochron, suggesting these two extractions released a mixture of both Ar components.

below), but with a considerably higher $^{40}\text{Ar}/^{36}\text{Ar}$ intercept. The FG-Plag appears to have released over intermediate extraction temperatures a trapped ^{40}Ar and ^{36}Ar component with $^{40}\text{Ar}/^{36}\text{Ar} \sim 10^3$, which was not present in the other extractions, nor in CG-Plag.

Because we use $^{36}\text{Ar}_{\text{cos}}$ and ^{37}Ar in most of the isochrons, the $^{40}\text{Ar}/^{36}\text{Ar}_{\text{cos}}$ and $^{40}\text{Ar}/^{37}\text{Ar}$ intercept ratios represent mixed components and have no physical meaning. However, the isochron slope still identifies any excess ^{40}Ar that is associated in the lattice with ^{40}Ar from in situ decay. The total amount of $^{40}\text{Ar}_{\text{xs}}$ in CG-Plag relative to an age of 170 Myr, is calculated to be $15.7 \times 10^{-7} \text{ cm}^3/\text{g}$. The total Ar-Ar age of CG-Plag is 242 Myr. Taking this total age, an isochron age of 217 Myr, and the formation age of ~ 170 Myr, we calculate that about 50% of the total $^{40}\text{Ar}_{\text{xs}}$ is a component defined by the isochron slope and very strongly correlated in the lattice with K and ^{40}Ar formed in situ by radioactive decay. The origin of the remaining $\sim 50\%$ of the excess ^{40}Ar is unclear. It may be in part terrestrial Ar acquired by the grains during mineral preparation, or Martian Ar trapped in inclusions or other phases within the minerals.

Although not as well defined as the CG isochron, the two separate isochrons for FG-Plag (Fig. 3) give similar isochron ages of ~ 300 Myr. A $^{40}\text{Ar}/^{37}\text{Ar}$ versus $^{39}\text{Ar}/^{37}\text{Ar}$ isochron for all FG-Plag data ($R^2 = 0.96$; not shown) suggests an age of ~ 350 Myr. Because the lower isochron in Fig. 3 ($R^2 = 0.987$) consists of both $^{36}\text{Ar}_{\text{cos}}$ (54–98% ^{39}Ar release) and $^{36}\text{Ar}_{\text{trap}}$ (0–25% ^{39}Ar release), the $^{40}\text{Ar}/^{36}\text{Ar}$ intercept for this isochron, which may not be significantly different from zero, may have no physical meaning. The total $^{40}\text{Ar}_{\text{xs}}$ in FG-Plag, relative to an age of 170 Myr, is $23.4 \times 10^{-7} \text{ cm}^3/\text{g}$. Relative to the slightly different isochron ages obtained by normalizing to $^{36}\text{Ar}_{\text{cos}}$ or ^{37}Ar , $\sim 70\%$ or $\sim 100\%$, respectively, of the total excess ^{40}Ar is

contained in the isochrons and is correlated with lattice K and in situ decay ^{40}Ar . The second, upper isochron for FG-Plag (Fig. 3) represents $\sim 25\%$ of the excess ^{40}Ar and suggests a trapped $^{40}\text{Ar}/^{36}\text{Ar}$ ratio of ~ 1000 . The excess Ar defined by the intercept could be Martian atmosphere present in a shock-produced phase which contaminates the feldspar separate.

Pyroxene

The Ar-Ar age spectra for one pyroxene separate of Zagami CG phase and two pyroxene separates of Zagami FG phase are similar and are shown in Fig. 4. In all three spectra, the first $\sim 60\text{--}75\%$ of the ^{39}Ar releases show relatively high K/Ca ratios and relatively low Ar ages, which resemble those measured in plagioclase separates. For higher temperature extractions, the K/Ca ratio decreases by orders of magnitude and the Ar ages increase appreciably, up to ≥ 3 Gyr. We attribute the first $\sim 70\%$ of the ^{39}Ar releases to no more than a few percent of mesostasis and plagioclase contaminants in the pyroxene separates. The pyroxene phase degasses Ar in the last $\sim 25\%$ of the ^{39}Ar release. It is important to note that, whereas most of the ^{39}Ar in these samples degassed from the plagioclase contaminant, most of the total ^{40}Ar degassed from the pyroxene. For example, for both CG-Px2 and FG-Px2 the Ar ages are relatively constant at < 0.4 Gyr until $\sim 75\%$ of the ^{39}Ar is released, at which point the ages sharply rise. In contrast, 74% of the total ^{40}Ar in FG-Px2 was released above 75% ^{39}Ar release, and 66% of the total ^{40}Ar in FG-Px2 was released above 81% of the ^{39}Ar release. Thus, the great majority of $^{40}\text{Ar}_{\text{xs}}$ in these separates is located in the pyroxene phase.

In utilizing isochron plots for these pyroxene separates, the problem of differentiating cosmogenic ^{36}Ar from trapped

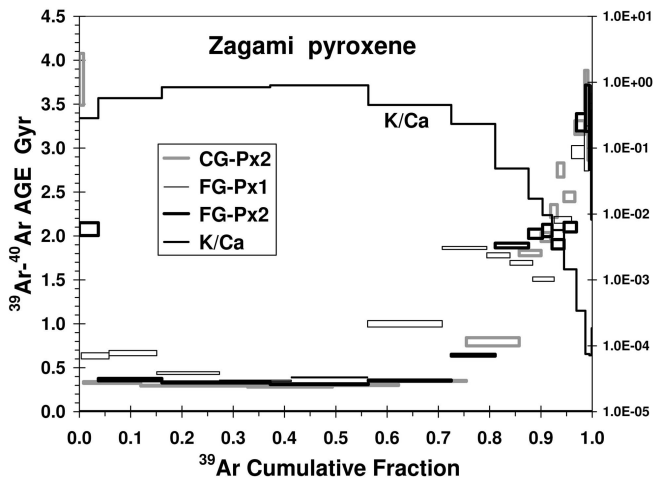


Fig. 4. ^{39}Ar - ^{40}Ar ages (rectangles, left Y-axis) plotted against cumulative ^{39}Ar release for stepwise temperature extractions of three pyroxene separates from CG and FG Zagami phases. K/Ca ratios (right Y-axis) for the FG-Px2 analysis are also shown.

^{36}Ar is more pronounced than for the plagioclase separates. This is illustrated in Fig. 5, which shows that $^{36}\text{Ar}/^{37}\text{Ar}$ ratios from FG-Px2 vary by two orders of magnitude and anti-correlate with the $^{40}\text{Ar}/^{39}\text{Ar}$ ratios. (The other two pyroxenes give similar plots.) Because most of the ^{37}Ar produced in the reactor from Ca is released from the pyroxene phase, not the minor plagioclase contaminant, pyroxene phase data plot to the upper left, where cosmogenic ^{36}Ar greatly dominates over trapped ^{36}Ar . Thus, we examined in isochron plots only that Ar released from the pyroxene phase of these separates. First we use $^{36}\text{Ar}_{\text{cos}}$ obtained by correcting for trapped ^{36}Ar using the lowest measured $^{36}\text{Ar}/^{37}\text{Ar}$ ratios. All three pyroxene separates give similar $^{36}\text{Ar}_{\text{cos}}$ concentrations of $\sim 2.4\text{--}2.9 \times 10^{-9} \text{ cm}^3/\text{g}$. Although our plagioclase and pyroxene separates contain similar Ca concentrations, the presence of another target element, Fe, in pyroxene probably produced a greater amount of $^{36}\text{Ar}_{\text{cos}}$. These isochron plots are shown in Fig. 6. As before, the $^{40}\text{Ar}/^{36}\text{Ar}$ intercepts do not characterize a specific component. Two of the intercepts are within uncertainty of zero, indicating that all the $^{40}\text{Ar}_{\text{xs}}$ is correlated with ^{39}Ar , and the third intercept has a relatively small value. We also constructed isochron plots by normalizing to ^{37}Ar . These isochrons are very similar to those in Fig. 6. The apparent isochron ages for FG-Px1, FG-Px2, and CG-Px2, normalized to ^{37}Ar and weighed by individual ratio uncertainties, are $1750 \pm 22 \text{ Myr}$, $1922 \pm 37 \text{ Myr}$, and $1991 \pm 40 \text{ Myr}$, respectively. Most of the ^{40}Ar released from these pyroxene phases is $^{40}\text{Ar}_{\text{xs}}$.

Concentrations of $^{40}\text{Ar}_{\text{xs}}$

Table 1 summarizes concentrations of $^{40}\text{Ar}_{\text{xs}}$ in the two plagioclase and three pyroxene separates analyzed. Each value was calculated by subtracting from measured ^{40}Ar the

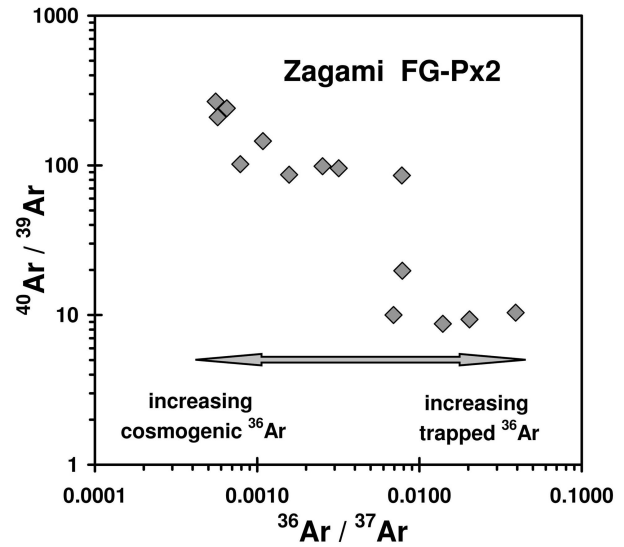


Fig. 5. Plot of $^{40}\text{Ar}/^{39}\text{Ar}$ against $^{36}\text{Ar}/^{37}\text{Ar}$ for FG-Px2 extractions, demonstrating that most of the $^{36}\text{Ar}_{\text{cos}}$ and $^{40}\text{Ar}_{\text{xs}}$ were degassed together from the higher temperature pyroxene phase.

amount of $^{40}\text{Ar}^*$ that would be produced in situ, assuming a Zagami crystallization age of 170 Myr. The concentrations of $^{40}\text{Ar}_{\text{xs}}$ in the five separates are similar at $\sim 1\text{--}2 \times 10^{-6} \text{ cm}^3/\text{g}$, and the $^{40}\text{Ar}_{\text{xs}}$ expressed as a percentage of the total ^{40}Ar varies by a factor of three. There appears to be no significant difference in $^{40}\text{Ar}_{\text{xs}}$ between CG and FG phases nor between plagioclase and pyroxene. If we subtract that $^{40}\text{Ar}_{\text{xs}}$ in FG-Plag, released at intermediate temperatures, which shows a trapped $^{40}\text{Ar}/^{36}\text{Ar} \cong 1000$ and which may be Martian atmosphere (Fig. 3), the overall variation in $^{40}\text{Ar}_{\text{xs}}$ becomes even less. Although Zagami FG was observed to have higher $^{87}\text{Sr}/^{86}\text{Sr}$ ratios than CG, implying a greater crustal component (Nyquist et al. 2006a), such a difference is not readily apparent in $^{40}\text{Ar}_{\text{xs}}$.

ORIGIN OF EXCESS ^{40}Ar

There are three conceivable origins for $^{40}\text{Ar}_{\text{xs}}$ in these Zagami mineral separates: 1) shock-implanted Martian atmospheric Ar; 2) Zagami is really much older than $\sim 170 \text{ Myr}$ and ^{40}Ar from in situ decay was not completely degassed by a thermal event; and 3) excess ^{40}Ar acquired from the magma or from rock digested into the magma prior to crystallization. We discount terrestrial atmospheric Ar, except possibly for the first few extractions, which tended to release only small fractions of the total $^{40}\text{Ar}_{\text{xs}}$. We now examine the viability of each of these three possible origins of $^{40}\text{Ar}_{\text{xs}}$.

Martian Atmosphere

Almost all of the several Martian shergottites Ar-Ar dated (Bogard and Garrison 1999 and unpublished data;

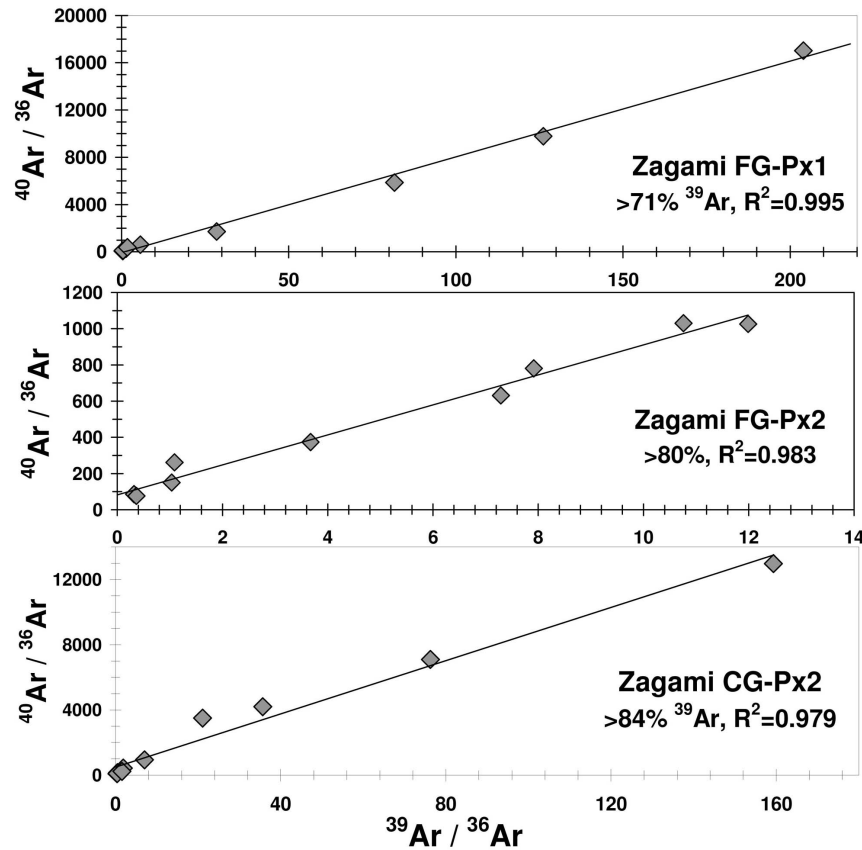


Fig. 6. Isochron plots of $^{40}\text{Ar}/^{36}\text{Ar}$ versus $^{39}\text{Ar}/^{36}\text{Ar}$ for pyroxene phases (defined by the range of ^{39}Ar releases indicated) of three Zagami pyroxene separates. Argon-36 is cosmogenic. Values for unweighed goodness of fit, R^2 , are also shown. Apparent Ar-Ar “ages” are ~ 1.8 – 1.9 Gyr.

Table 1. Excess ^{40}Ar in Zagami mineral separates (units 10^{-7} cm 3 STP/g and percent of total ^{40}Ar).

Phase	$^{40}\text{Ar}_{\text{xs}}$	% total
CG-Plag	15.7	32
FG-Plag ¹	23.4 (17.9)	54
CG-Px2	10.8	85
FG-Px2	9.2	86
FG-Px1	15.3	89

¹Second value for FG-Plag subtracts the trapped component with $^{40}\text{Ar}/^{36}\text{Ar} = 1000$.

Walton et al. 2007) show significant $^{40}\text{Ar}_{\text{xs}}$ compared to their Sm-Nd ages. For some shergottites, we purposely chose samples that exhibited high shock levels and/or consisted of impact melt. These samples clearly give evidence of trapped noble gases that resemble the Martian atmosphere in composition (Bogard and Garrison 1998, 1999). In contrast, Zagami experienced a relatively low shock level. Fritz et al. (2005) reported shock levels of several shergottites to have been in the range of ~ 10 – 45 GPa, which correspond to temperature increases of ~ 10 °C to ~ 800 °C. These estimated shock pressures were obtained from observed changes in mineral characteristics produced by shock, combined with

equations of state for relevant materials, and generally confirmed by artificial shock experiments (Stöffler et al. 1988; Sharp and DeCarli 2006; and references therein). Zagami is reported to have experienced shock of ~ 30 GPa and a temperature rise of ~ 70 °C (Fritz et al. 2005). Zagami also has been reported to contain $<1\%$ and $\sim 2\%$ shock melt present in veins and pockets (McCoy et al. 1992; Walton et al. 2007). To our knowledge, our Zagami samples did not contain any shock melt. More importantly, five mineral separates obtained from two different pieces of Zagami give similar concentrations of $^{40}\text{Ar}_{\text{xs}}$. If one of our initial samples contained impact glass, we might expect that glass to be concentrated in a particular mineral separate and not be equally present in others. Also, we would not expect $^{40}\text{Ar}_{\text{xs}}$ in shock glass to be uniformly distributed through the mineral lattice of each separate in proportion to ^{39}Ar , as we argue above from the isochron plots. Finally, we find minimum evidence that $^{40}\text{Ar}_{\text{xs}}$ is closely associated with trapped ^{36}Ar , unlike our previous study on strongly shocked shergottites, where these two components were strongly correlated and indicated Martian atmospheric $^{40}\text{Ar}/^{36}\text{Ar}$ ratios of ~ 1800 (Bogard and Garrison 1999). Thus, we reject the possibility that $^{40}\text{Ar}_{\text{xs}}$ in Zagami arose by shock implantation of the Martian atmosphere.

Residue from Thermal Degassing of an Old Zagami

The Ar-Ar chronometer is known to be reset more easily by thermal events in a wide variety of materials, when compared to the Sm-Nd, Rb-Sr, and U-Pb chronometers (e.g., Bogard 1995 and references therein; Dickin 1995). Yet, in all shergottites analyzed, the Ar-Ar age is oldest, often by a substantial margin (e.g., Garrison and Bogard 2001; Nyquist et al. 2001; Walton et al. 2007). At highest extraction temperatures, the apparent Ar-Ar ages of Zagami pyroxene rise to 3 Gyr and above (Fig. 4), and for this $^{40}\text{Ar}_{\text{xs}}$ to be a diffusion remnant of ^{40}Ar formed in situ would imply a Zagami formation age at least this old. A cogent reason would be required for the true crystallization age of Zagami to be older than the Sm-Nd and Rb-Sr ages and also older than the apparent Ar-Ar ages. Bouvier et al. (2005, 2007), using Pb-Pb isotopic data from Zagami and a few other shergottites, suggested that these shergottites actually formed 4.0 Gyr ago and that the Sm-Nd and Rb-Sr chronometers of some minerals, particular phosphates, were reset by acidic aqueous solutions percolating through the Martian surface. However, other chronologists have strongly argued for young ages for the shergottites (Nyquist 2006; Nyquist et al. 2001, 2006b; Misawa et al. 2006; Herd et al. 2007; Shih et al. 2007; Jones 2007; Bogard and Park 2007b). Experimental studies suggest that pyroxene would be more strongly weathered than plagioclase in aqueous solutions ranging from moderately acidic to moderately basic (McAdam et al. 2006). Further, plagioclase separates help define the old Pb isochron age argued by Bouvier et al. (2005), implying that plagioclase could not be significantly weathered. Partial degassing of an old Zagami also would have to explain a required movement of radiogenic argon produced in the K-rich plagioclase into the K-poor pyroxene so as to produce the roughly equal concentrations we observe in these minerals, all achieved without any textural evidence for alteration.

Although the Ar-Ar age of Zagami plagioclase is unlikely to have been reset by acidic weathering on Mars, we here examine the possibility that Zagami did, in fact, form 4 Gyr ago, and that most of its radiogenic ^{40}Ar was degassed by some thermal event, the most probable being the event that ejected it from Mars ~3 Myr ago (Nyquist et al. 2001). To make this examination, we first consider the diffusion coefficient, D/a^2 , for Ar measured in Zagami plagioclase, where D is diffusivity and a is gas diffusion distance before loss, generally taken as the grain diameter. Then, we incorporate this diffusion parameter into a thermal cooling model for Zagami. Figure 7 shows an Arrhenius diffusion plot for ^{39}Ar (McDougall and Harrison 1999) calculated from all of the stepwise degassing steps obtained on Zagami CG-Plag using the equations given by Fechtig and Kalbitzer (1966). The strongly linear trend indicates that Ar diffusion in this sample occurred from a single diffusion domain, and that the diffusion trend can be extrapolated to lower temperature with reasonable confidence. The extrapolated value of the diffusion

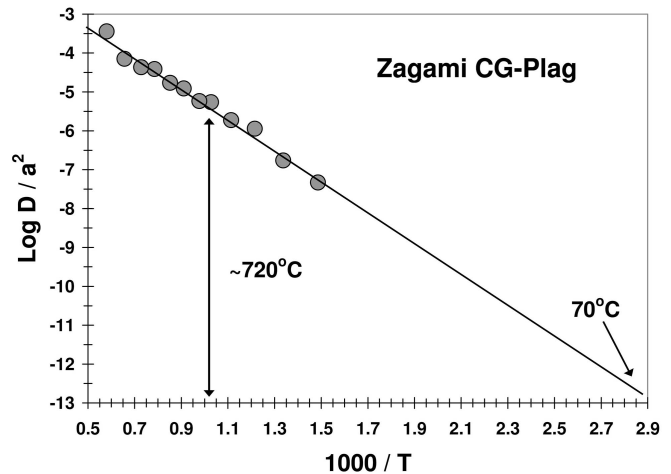


Fig. 7. Arrhenius diffusion plot, D/a^2 versus reciprocal temperature in Kelvin, for ^{39}Ar released in all extractions of Zagami CG plagioclase.

coefficient, D/a^2 , at the Zagami shock-heating temperature of 70 °C, (Fritz et al. 2005), is about 10^{-13} s^{-1} .

We envision that Zagami was shock-heated to ~70 °C (Fritz et al. 2005) when it was ejected into space ~3 Myr ago (Eugster et al. 1997). For a cooling body, the ratio of some temperature, T , to an initial temperature, T_0 , has an exponential relationship to the elapsed time, t , the characteristic thermal diffusivity of the body, k , the distance, r , internal heat must diffuse to reach the surface of the body and escape, and a constant that represents the geometrical shape of the body (Carslaw and Jaeger 1959). We adopt $k = 0.004 \text{ cm}^2/\text{s}$, which is a value typical for solid silicates under low gas-phase pressures (Carslaw and Jaeger 1959; Horai and Winkler 1976); we assume a Zagami surface temperature in space of 0 °C (Ghosh and McSween 1998); and we assume the geometry of a sphere for Zagami in space. Figure 8 shows the calculated relationship between the radius of a cooling silicate sphere (left Y-axis) and elapsed time for the two cases where the ratio T/T_0 has the values of 0.9 and 0.5. The thermal diffusion constant is relatively independent on temperature (Horai and Winkler 1976), whereas the gas diffusion coefficient is very temperature dependent (Fig. 7). Thus, most of the Ar diffusion and loss would occur during the early stages of thermal cooling (Bogard et al. 1979).

The analytic form of gas diffusion is analogous to that for heat diffusion. The ratio of some gas concentration, C , to some initial concentration, C_0 , is exponentially proportional to the elapsed time, t , the gas diffusivity, D , and the distance the gas must diffuse to be lost, which is generally taken to be the grain diameter, a (Crank 1956). The elapsed time, t , is the same in both the thermal and gas diffusion relationships. Thus, Fig. 8 also shows the Ar diffusion parameter, D/a^2 (right Y-axis), plotted against elapsed time for the two cases that fractional loss of ^{40}Ar , F , is 50% and 95% (Fechtig and Kalbitzer 1966).

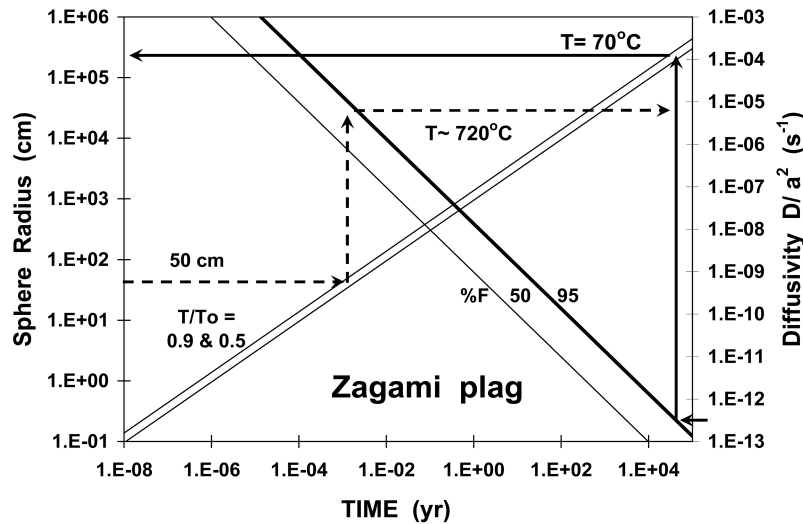


Fig. 8. Combined model for radius of spherical object undergoing thermal cooling (left scale) and argon diffusivity (right scale) as a function of time in years. Diagonal lines indicate decreasing temperature ratios, $T/T_0 = 0.9$ and 0.5 , and fractional diffusion loss of Ar, $F = 50\%$ and 90% . Solid arrows show relationship between Ar diffusion in Zagami CG plagioclase heated to $70\text{ }^\circ\text{C}$ and required Mars-ejected size. Dashed arrows give parameters for a more reasonable Mars-ejected size.

If Zagami crystallized 4 Gyr ago and lost most of its ^{40}Ar ~ 3 Myr ago during shock-heating to $70\text{ }^\circ\text{C}$, then the 242 Myr total Ar-Ar “age” of the CG-Plag implies that $\sim 98\%$ of the original ^{40}Ar was degassed. If the degassing time were 170 Myr ago, then $>99\%$ of the original ^{40}Ar would have been degassed. From Fig. 7, we adopt a D/a^2 value of 3×10^{-13} for heating Zagami CG-Plag to $70\text{ }^\circ\text{C}$, and we find the corresponding location on the $F = 95\%$ diffusion loss line (Fig. 8), which also corresponds to $t \approx 2 \times 10^4$ years. This time for 95% gas loss also defines the characteristic thermal cooling time, which corresponds to a position on the thermal cooling lines for $T/T_0 = 0.9\text{--}0.5$ (illustrated by the series of solid arrows). Reading this position on the left Y-axis gives the required diameter of a sphere in space that would cool this slowly from an initial temperature of $70\text{ }^\circ\text{C}$. This analysis yields the result that, for Zagami CG-Plag to have formed 4 Gyr ago and to have lost $>98\%$ of its original ^{40}Ar by shock-heating to $70\text{ }^\circ\text{C}$ when ejected into space, then its ejected mass is required to have been on the order of a kilometer in radius. This obviously was not the case. Even if Zagami formed much later than 4 Gyr ago and lost, e.g., 50% of its ^{40}Ar , its ejected mass is required to have been hundreds of meters in radius.

Zagami, with a mass of ~ 18 kg, is the largest Martian meteorite recovered. From theoretical models, Head et al. (2002) estimated the Mars-ejected size of Zagami to have been 0.28 m. Concentrations of ^{80}Kr in Zagami produced by neutron capture prior to impact ejection suggest a minimum ejected radius of 0.23 m (Eugster et al. 2002). We can use Fig. 8 and a conservative upper limit of 50 cm radius (~ 1500 kg) for the size for Mars-ejected Zagami to discern what shock heating temperature for Zagami would be required under the same scenario discussed above. We see

that this assumption (Fig. 8, dashed arrows) gives a value for D/a^2 of $\sim 3 \times 10^{-6}$, which from Fig. 7 corresponds to a temperature of $\sim 720\text{ }^\circ\text{C}$. Smaller Zagami ejected masses would have to be heated proportionally hotter. It seems very unlikely that the shock-heating temperature of Zagami has been underestimated by an order of magnitude. In the compilation of shock temperatures of shergottites by Fritz et al. (2005), only ALH 77005, shocked to ~ 45 GPa, was heated to a temperature near this value.

We also considered the possibility that the impact event that heated Zagami to $\sim 70\text{ }^\circ\text{C}$ was not the Mars-ejection event, but a much larger impact that occurred much earlier, possibly ~ 170 Myr ago (Mittlefehldt et al. 1999). If Zagami were buried about a kilometer deep within an enormous ejecta blanket, but heated only to $\sim 70\text{ }^\circ\text{C}$, its cooling rate could, in principle, be consistent with our thermal model. However, this scenario seems unlikely for two reasons. First, it seems likely that deep portions of such a large ejecta would be heated to much more than $70\text{ }^\circ\text{C}$. Second, if this impact left Zagami buried at such a large depth, a second, later impact would be required to bring it nearer to the Martian surface, and then a third impact would be required to eject it from Mars (Head et al. 2002).

Thus, we conclude that the Ar-Ar data for Zagami do not permit its crystallization age to be anywhere near as old as 4 Gyr, and that the $^{40}\text{Ar}_{\text{xs}}$ in Zagami does not represent ^{40}Ar formed in situ from the decay of ^{40}K and later partially degassed. We consider this to be a strong argument against the suggestion by Bouvier et al. (2005) that Zagami crystallized 4 Gyr ago. Rather, we conclude that Zagami crystallized ~ 0.17 Gyr ago, as given by its Sm-Nd and Rb-Sr ages, and that it contains small amounts of excess ^{40}Ar in its constituent igneous minerals, whose likely origin we consider below.

Implications of Magmatic $^{40}\text{Ar}_{\text{xs}}$ for Zagami Petrogenetic History

Our remaining explanation for $^{40}\text{Ar}_{\text{xs}}$ in Zagami is that it was inherited from the source magma or from crustal rock assimilated into the magma. We now examine the implications of such an origin. Terrestrial MORBs (mid-ocean ridge basalts) and OIBs (ocean island basalts) typically contain $\sim 10^{-8}$ to 10^{-5} cm^3/g of $^{40}\text{Ar}_{\text{xs}}$ (Burnard et al. 1997; Niedermann et al. 1997; Shibata et al. 1998; Trierloff et al. 2003), which is comparable to the Zagami $^{40}\text{Ar}_{\text{xs}}$ concentration of $\sim 1 \times 10^{-6}$ cm^3/g (Table 1). Recent comprehensive studies of the mineral-melt distribution coefficients for Ar into olivine and clinopyroxene give values of ~ 0.0011 for each (Brooker et al. 2003; Heber et al. 2007). This implies that the Zagami melt from which the meteorite crystallized contained an ^{40}Ar concentration of $\sim 10^{-3}$ cm^3/g . The solubilities of Ar in rock melts of various compositions are relatively well known at $\sim 1\text{--}30 \times 10^{-5}$ $\text{cm}^3/\text{g}\text{-bar}$ and $\sim 5 \times 10^{-5}$ $\text{cm}^3/\text{g}\text{-bar}$ for basalt melt (Heber et al. 2007; Shibata et al. 1998). This would imply that the partial pressure of ^{40}Ar when Zagami crystallized was about 20 bar. By comparison, the lithostatic pressure on Mars is ~ 1 kbar at the >7 km depth, at which Zagami crystallization is thought to have begun (McCoy et al. 1992, 1999; McSween et al. 2001). If the magma possessed a K concentration of 0.1%, the same value as Zagami whole rock, then it would require more than 5 Gyr for this much ^{40}Ar to accumulate. The magma would have to have K $\sim 2\%$ to generate this much ^{40}Ar in <4 Gyr. This suggests either that ^{40}Ar in the Zagami magma was concentrated from a much larger volume than the magma source rock by degassing into the magma chamber, or that a K-rich, old crustal material was assimilated into the magma, bringing much of the ^{40}Ar with it. This is the possibility offered by Nyquist et al. (2006a) to explain different $^{87}\text{Sr}/^{86}\text{Sr}$ ratios for CG and FG Zagami. Jones (1989) also concluded that shergottites underwent large amounts of assimilation and/or fractional crystallization. Such crustal assimilation would have to occur early in the Zagami crystallization sequence in order to produce pyroxene and plagioclase minerals with similar $^{40}\text{Ar}_{\text{xs}}$ concentrations.

During fractional crystallization the $^{40}\text{Ar}_{\text{xs}}$ concentration in Zagami magma might be expected to increase as minerals precipitate, and the last crystallizing phase (plagioclase/mesostasis) might be expected to show much higher $^{40}\text{Ar}_{\text{xs}}$ concentration than the early crystallizing pyroxene. We see from Table 1 that this is not the case. Further, within a factor of two, there is no significant difference in $^{40}\text{Ar}_{\text{xs}}$ concentrations for the CG and FG phases, which are thought to contain different amounts of the early crystallizing minerals. This observation may indicate that ^{40}Ar was lost from the magma so as to maintain a constant concentration as the magma rose toward the surface, pressure was released, and crystallization proceeded. This is the same process postulated by McSween et al. (2001) for water in the Shergotty magma. These authors

suggested the original Shergotty magma contained 1.8% water at depth and that most of this was lost as the magma rose toward the surface. The Zagami and Shergotty meteorites are both low in water content (Jones 2004, and references therein). Whether $^{40}\text{Ar}_{\text{xs}}$ in Zagami arose from mantle melting or crustal assimilation, whether Zagami magma was wet or dry, the Zagami magma appears to have possessed, then lost significant amounts of radiogenic ^{40}Ar . This scenario is consistent with the Martian crust and upper mantle being still relatively rich in volatiles (Bogard et al. 2001), and it seems consistent with suggested petrogenetic formation models of both Zagami and Shergotty.

SUMMARY AND CONCLUSIONS

Ar-Ar analyses of plagioclase and pyroxene mineral separates from both coarse- and fine-grained phases of the Zagami Martian shergottite all give $^{39}\text{Ar}\text{-}^{40}\text{Ar}$ ages higher than the Sm-Nd and Rb-Sr ages of ~ 170 Myr (Nyquist et al. 2001; Borg et al. 2005). Isochron plots of $^{40}\text{Ar}/^{36}\text{Ar}$ versus $^{39}\text{Ar}/^{36}\text{Ar}$ and $^{40}\text{Ar}/^{37}\text{Ar}$ versus $^{39}\text{Ar}/^{37}\text{Ar}$ for these data also yield ages higher than these other radiometric ages. The amounts of excess ^{40}Ar ($^{40}\text{Ar}_{\text{xs}}$), calculated relative to the amount of ^{40}Ar that would decay in situ over ~ 170 Myr, is $\sim 1\text{--}2 \times 10^{-6}$ cm^3/g and is similar for each sample analyzed. A substantial fraction of this $^{40}\text{Ar}_{\text{xs}}$ in each sample is associated with the isochron, indicating that it is distributed through the lattice and not contained in impact glass. The low shock pressure of Zagami, the similarity of $^{40}\text{Ar}_{\text{xs}}$ concentrations in each analyzed sample, the distribution of $^{40}\text{Ar}_{\text{xs}}$ through the lattice, and minimal evidence that trapped ^{36}Ar is closely associated with $^{40}\text{Ar}_{\text{xs}}$, all indicate that this excess $^{40}\text{Ar}_{\text{xs}}$ is not Martian atmosphere directly introduced into the meteorite.

We also argue that $^{40}\text{Ar}_{\text{xs}}$ does not result from ^{40}K decay inside Zagami over a much longer time period, e.g., 4 Gyr, and was only partially degassed by a recent thermal event. Such a scenario would seemingly require ^{40}Ar from in situ decay in plagioclase, which contains most of the K, to migrate into pyroxene in order to produce roughly equal concentrations of $^{40}\text{Ar}_{\text{xs}}$. We also can rule out partial ^{40}Ar degassing based on diffusion properties. The shock-heating temperature rise for Zagami has been determined to be ~ 70 °C (Fritz et al. 2005). Using Ar diffusion characteristics measured for Zagami plagioclase and a model relating Ar diffusion loss with thermal cooling of a body in space, we examine a scenario whereby Zagami might be 4 Gyr old and was strongly degassed of its ^{40}Ar by the CRE event that launched it into space ~ 3 Myr ago. With these assumptions, cooling must have been exceedingly slow and the ejected size of Zagami would have been impossibly large (~ 1 km). A reasonable estimated size for ejected Zagami (≤ 0.5 m) would require that Zagami was heated to ≥ 700 °C in order to lose most of its ^{40}Ar by diffusion while cooling in space. From this analysis, we

conclude that Zagami could not have crystallized 4 Gyr ago, but most likely formed much more recently, i.e., ~170 Myr ago.

Zagami (and Shergotty) experienced a complex and prolonged crystallization history, beginning at considerable depth (>7 km) and continuing as magma rose toward the surface and evolved in composition (McCoy et al. 1992, 1995, 1999; Lentz and McSween 2000; McSween et al. 2001). Although from this history one might expect the analyzed CG and FG Zagami mineral separates to contain different $^{40}\text{Ar}_{\text{xs}}$ concentrations, the Ar data presented in this study show no significant differences. We conclude that the most likely origin of $^{40}\text{Ar}_{\text{xs}}$ in Zagami is a radiogenic component inherited from the source magma or from crustal material assimilated into the magma early in Zagami crystallization history. Concentrations of $^{40}\text{Ar}_{\text{xs}}$ in Zagami are similar to those measured in terrestrial MORBs and OIBs, and literature data for Ar distribution coefficients for pyroxene and olivine relative to basaltic melt imply a relatively high initial partial pressure of ^{40}Ar in Zagami magma of ~20 bar at >7 km depth. This ^{40}Ar pressure indicates that the Zagami magma acquired extra ^{40}Ar , either by degassing from surrounding rock or from assimilation of old crustal rock relatively high in potassium. To maintain an approximately constant ^{40}Ar concentration in the rising magma, the ^{40}Ar may have been continually lost as pressure on the magma was released and Zagami crystallization proceeded. A similar scenario was suggested for water loss from the Shergotty magma (McSween et al. 2001). This origin of $^{40}\text{Ar}_{\text{xs}}$ in Zagami has implications for some other shergottites, which also contain ^{40}Ar concentrations above those predicted from their measured crystallization ages.

Acknowledgments—We thank L. Nyquist and C.-Y. Shih for the Zagami mineral separates. This work was supported by the NASA Cosmochemistry Program and by a fellowship from the NASA Postdoctoral Program to J. P. We appreciate constructive comments on the paper by L. Nyquist, E. Walton, and S. Kelley.

Editorial Handling—Dr. John Spray

REFERENCES

- Bogard D. D. 1995. Impact ages of meteorites: A synthesis. *Meteoritics* 30:244–268.
- Bogard D. D. and Johnson P. 1983. Martian gases in an Antarctic meteorite. *Science* 221:651–654.
- Bogard D. D. and Garrison D. H. 1998. Relative abundances of Ar, Kr, and Xe in the Martian atmosphere as measured in Martian meteorites. *Geochimica et Cosmochimica Acta* 62:1829–1835.
- Bogard D. D. and Garrison D. H. 1999. Argon-39—argon-40 “ages” and trapped argon in Martian shergottites, Chassigny, and Allan Hills 84001. *Meteoritics & Planetary Science* 34:451–473.
- Bogard D. D. and Park J. 2007a. Excess ^{40}Ar in the Zagami shergottite: Does it reveal crystallization history? (abstract). *Meteoritics & Planetary Science* 42:A21.
- Bogard D. D. and Park J. 2007b. Ar-Ar age of NWA-1460 and evidence for young formation ages of the shergottites (abstract #1096). 38th Lunar and Planetary Science Conference. CD-ROM.
- Bogard D. D., Husain L., and Nyquist L. E. 1979. ^{40}Ar - ^{39}Ar age of the Shergotty achondrite and implications for its post-shock thermal history. *Geochimica et Cosmochimica Acta* 43:1047–1055.
- Bogard D. D., Garrison D. H., Norman M., Scott E. R. D., and Keil K. 1995. ^{39}Ar - ^{40}Ar age and petrology of Chico: Large-scale impact melting of the L chondrite parent body. *Geochimica et Cosmochimica Acta* 59:1383–1400.
- Bogard D. D., Garrison D. H., and McCoy T. J. 2000. Chronology and petrology of silicates from IIE iron meteorites: Evidence of a complex parent body evolution. *Geochimica et Cosmochimica Acta* 64:2133–2154.
- Bogard D. D., Clayton R. N., Marti K., Owen T., and Turner G. 2001. Martian volatiles: Isotopic composition, origin, and evolution. In *Chronology and evolution of Mars*. Space Science Reviews, vol. 96. pp. 425–458.
- Borg L. E., Edmunson J. E., and Asmerom Y. 2005. Constraints on the U-Pb isotopic systematics of Mars inferred from a combined U-Pb, Rb-Sr, and Sm-Nd isotopic study of the Martian meteorite Zagami. *Geochimica et Cosmochimica Acta* 69:5819–5830.
- Bouvier A., Blichert-Toft J., Vervoort J. SD., and Albarède F. 2005. The age of SNC meteorites and the antiquity of the Martian surface. *Earth & Planetary Science Letters* 240:221–233.
- Bouvier A., Blichert-Toft J., Vervoort J. SD., and Albarède F. 2007. The conundrum of the age of shergottites (abstract #1683). 38th Lunar and Planetary Science Conference. CD-ROM.
- Brooker R. A., Du Z., Blundy J. D., Kelley S. P., Allan N. L., Wood B., Chamorro E. M., Wartho J. A., and Purton J. A. 2003. The “zero charge” partitioning behaviour of noble gases during mantle melting. *Nature* 423:738–740.
- Burnard P., Graham D., and Turner G. 1997. Vesicle-specific noble gas analysis of “popping rock”: Implications for primordial noble gases in Earth. *Science* 276:568–571.
- Carlsaw H. S. and Jaeger J. C. 1959. *Conduction of heat in solids*, 2nd ed. Oxford: Clarendon Press. 510 p.
- Crank J. 1956. *Mathematics of diffusion*. Oxford: Clarendon Press. 347 p.
- Dickin A. P. 1995. *Radiogenic isotope geology*. Cambridge: Cambridge University Press. 490 p.
- Eugster O., Weigel A., and Polnau E. 1997. Ejection times of Martian meteorites. *Geochimica et Cosmochimica Acta* 61:2749–2759.
- Eugster O., Busemann H., and Lorenzetti S. 2002. The pre-atmospheric size of Martian meteorites (abstract #1096). 33rd Lunar and Planetary Science Conference. CD-ROM.
- Fechtig H. and Kalbitzer S. 1966. The diffusion of argon in potassium-bearing solids. In *Potassium-argon dating*, edited by Schaeffer O. J. and Zähringer J. New York: Springer-Verlag. pp. 68–107.
- Fritz J., Artemieva N., and Greshake A. 2005. Ejection of Martian meteorites. *Meteoritics & Planetary Science* 40:1393–1411.
- Garrison D. H., Hamlin S., and Bogard D. D. 2000. Chlorine abundances in meteorites. *Meteoritics & Planetary Science* 35:419–429.
- Garrison D. H. and Bogard D. D. 2001. Argon-39 and argon-40 “ages” and trapped argon for three Martian shergottites (abstract). *Meteoritics & Planetary Science* 36:A62.
- Ghosh A. and McSween H. Y. 1998. A thermal model for the differentiation of asteroid 4 Vesta, based on radiogenic heating. *Icarus* 134:187–206.
- Head J. N., Melosh H. J., and Ivanov B. A. 2002. Martian meteorite launch: High-speed ejecta from small craters. *Science* 298:1752–1756.

- Heber V. S., Brooker R. A., Kelley S. P., and Wood B. J. 2007. Crystal-melt partitioning of noble gases (helium, neon, argon, krypton, and xenon) for olivine and clinopyroxene. *Geochimica et Cosmochimica Acta* 71:1041–1061.
- Herd C. D. K., Simonetti A., and Peterson N. D. 2007. In situ U-Pb geochronology of Martian baddeleyite by laser ablation MC-ICP-MS (abstract #1664). 38th Lunar and Planetary Science Conference. CD-ROM.
- Horai K. and Winkler J. L. 1976. Thermal diffusivity of four Apollo 17 rock samples. Proceedings, 7th Lunar Science Conference. *Geochimica et Cosmochimica Acta* (Suppl. 7):3181–3204.
- Jones J. H. 1989. Isotopic relationships among the shergottites, the nakhlites, and Chassigny. Proceedings, 19th Lunar and Planetary Science Conference. pp. 465–474.
- Jones J. H. 2004. The edge of wetness: The case for dry magmatism on Mars (abstract #1798). 35th Lunar and Planetary Science Conference. CD-ROM.
- Jones J. H. 2007. The shergottites are young (abstract). *Meteoritics & Planetary Science* 42:A77.
- Lentz R. C. F. and McSween H. Y. 2000. Crystallization of the basaltic shergottites: Insight from crystal size distribution (CSD) analysis of pyroxenes. *Meteoritics & Planetary Science* 41:919–927.
- Marti K., Kim J. S., Thakur A. N., McCoy T. J., and Keil K. 1995. Signatures of the Martian atmosphere in glass of the Zagami meteorite. *Science* 267:1981–1984.
- McAdam A. C., Zolotov M. Yu., Mironenko M. V., Leshin L. A., and Sharp T. G. 2006. Aqueous chemical weathering of a Mars analog lithology: Kinetic modeling for a ferrar dolerite composition (abstract #2363). 37th Lunar and Planetary Science Conference. CD-ROM.
- McCoy T. J., Taylor G. J., and Keil K. 1992. Zagami: Product of a two-stage magmatic history. *Geochimica et Cosmochimica Acta* 56:3571–3582.
- McCoy T. J., Wadhwa M., and Keil K. 1995. Zagami: Another new lithology and a complex near-surface magmatic history (abstract). 26th Lunar and Planetary Science Conference. pp. 925–926.
- McCoy T. J., Wadhwa M., and Keil K. 1999. New lithologies in the Zagami meteorite: Evidence for fractional crystallization of a single magma unit on Mars. *Geochimica et Cosmochimica Acta* 63:1249–1262.
- McDougall I. and Harrison T. M. 1999. *Geochronology and thermochronology by the $^{40}\text{Ar}/^{39}\text{Ar}$ method*. 2nd ed. New York: Oxford University Press. 269 p.
- McSween H. Y., Grove T. L., Lentz R. C., Dann J. C., Holzheid A. H., Riciputi L. R., and Ryan J. G. 2001. Geochemical evidence for magmatic water within Mars from pyroxenes in the Shergotty meteorite. *Nature* 409:487–490.
- Mikouchi T., Miyamoto M., and McKay G. A. 1999. The role of undercooling in producing igneous zoning trends in pyroxenes and maskelynites among basaltic Martian meteorites, *Earth & Planetary Science Letters* 173:235–256.
- Misawa K., Yamada K., Nakamura N., Kondorosi G., Yamashita K., and Premo W. R. 2006. Sm-Nd isotopic systematics of Iherzolitic shergottite Yamato-793605 (abstract #1892). 37th Lunar and Planetary Science Conference. CD-ROM.
- Mittlefehldt D. W., Lindström D. J., Lindström M. M., and Martinez R. R. 1999. An impact-melt origin for lithology A of Martian meteorite Elephant Moraine A79001. *Meteoritics & Planetary Science* 34:357–367.
- Niedermann S., Bach W., and Erzinger J. 1997. Noble gas evidence for a lower mantle component in MORBs from the Southern East Pacific Rise: Decoupling of helium and neon isotopic systematics. *Geochimica et Cosmochimica Acta* 61:2697–2715.
- Nyquist L. E. 2006. Martian meteorite ages and implications for Martian cratering history (abstract #6010). Workshop on Surface ages and Histories: Issues In Planetary Chronology. CD-ROM.
- Nyquist L. E., Bogard D. D., Shih C.-Y., Greshake A., Stöffler D., and Eugster O. 2001. Ages and geological histories of Martian meteorites. In *Chronology and evolution of Mars*. Space Science Reviews, vol. 96. pp. 105–164.
- Nyquist L. E., Shih C.-Y., and Reese Y. 2006a. Initial isotopic heterogeneities in Zagami: Evidence of a complex magmatic history (abstract). *Meteoritics & Planetary Science* 41:A135.
- Nyquist L. E., Shih C.-Y., Reese Y., and Irving A. J. 2006b. Concordant Rb-Sr and Sm-Nd ages for NWA 1460: A 340 Ma old basaltic shergottite related to Iherzolitic shergottites (abstract #1723). 37th Lunar and Planetary Science Conference. CD-ROM.
- Park J. 2005. Noble gas study of Martian meteorites: New insights on Mars. Ph.D. thesis, University of Tokyo, Tokyo, Japan.
- Park J., Okazaki R., and Nagao K. 2003. Noble gas studies of Martian meteorites: Dar al Gani 476/489, Sayh al Uhaymir 005/060, Dhofar 019, Los Angeles 001, and Zagami (abstract #1213). 34th Lunar and Planetary Science Conference. CD-ROM.
- Schwenzer S. P., Herrmann S., Mohapatra R. K., and Ott U. 2007. Noble gases in mineral separates from three shergottites: Shergotty, Zagami, and EETA79001. *Meteoritics & Planetary Science* 42:387–412.
- Sharp T. C. and DeCarli P. S. 2006. Shock effects in meteorites. In *Meteorites and the early solar system II*, edited by Lauretta D. S. and McSween H. Y. Jr. Tucson: The University of Arizona Press. pp. 653–677.
- Shibata T., Takahashi E., and Matsuda J. 1998. Solubility of neon, argon, krypton, and xenon in binary and ternary silicate systems: A new view on noble gas solubility. *Geochimica et Cosmochimica Acta* 62:1241–1253.
- Shih C.-Y., Nyquist L. E., and Reese Y. 2007. Rb-Sr and Sm-Nd isotopic studies of Martian depleted shergottite SaU 094/005 (abstract #1745). 38th Lunar and Planetary Science Conference. CD-ROM.
- Stöffler D., Bischoff A., Buchwald U., and Rubin A. E. 1988. Shock effects in meteorites. In *Meteorites and the early solar system*, edited by Kerridge J. F. and Matthews M. S. Tucson: The University of Arizona Press. pp. 165–205.
- Trieloff M., Falter M., and Jessberger E. K. 2003. The distribution of mantle and atmospheric argon in oceanic basalt glasses. *Geochimica et Cosmochimica Acta* 67:1229–1245.
- Terrilini D., Eugster O., Burger M., Jakob A., and Krähenbühl U. 1998. Noble gases and chemical composition of Shergotty mineral fractions, Chassigny, and Yamato-793605: The trapped argon-40/argon-39 ratio and ejection times of Martian meteorites. *Meteoritics & Planetary Science* 33:677–684.
- Walton E. L., Kelly S. P., and Spray J. G. 2007. Shock implantation of Martian atmospheric argon in four basaltic shergottites: A laser probe $^{40}\text{Ar}/^{39}\text{Ar}$ investigation. *Geochimica et Cosmochimica Acta* 71:497–520.
- Williamson J. H. 1968. Least-squared fitting of a straight line. *Canadian Journal of Physics* 46:1845–1847.

APPENDIX

Table A1. Appendix of argon isotopic data. Columns from left to right give extraction temperature, ^{39}Ar concentration in $10^{-9} \text{ cm}^3\text{STP/g}$, age in Myr, K/Ca ratio, and Ar isotopic ratios normalized to ^{39}Ar . Uncertainties are given beneath the age and all ratios.

Temp. (°C)	^{39}Ar (cc/g)	Age (Myr)	K/Ca ±	40/39 ±	38/39 ±	37/39 ±	36/39 ±
Zagami FG-Plag, 8.0 mg							
300	0.7	4716	0.8623	583.06	1.259	0.58	1.8606
		202	0.1077	70.25	0.167	0.07	0.2335
400	7.5	412	0.9059	11.82	0.176	0.55	0.0228
		12	0.0324	0.39	0.009	0.02	0.0035
475	14.5	344	0.8318	9.68	0.122	0.60	0.0222
		10	0.0268	0.29	0.005	0.02	0.0023
550	20.2	294	0.7842	8.15	0.109	0.64	0.0078
		5	0.0157	0.14	0.003	0.01	0.0012
600	23.7	297	0.5101	8.25	0.130	0.98	0.0041
		4	0.0083	0.10	0.003	0.02	0.0009
625	21.3	308	0.3667	8.59	0.131	1.36	0.0044
		4	0.0061	0.11	0.003	0.02	0.0009
650	18.7	331	0.2908	9.29	0.133	1.72	0.0046
		4	0.0050	0.13	0.004	0.03	0.0010
675	20.0	416	0.1946	11.95	0.146	2.57	0.0057
		23	0.0124	0.74	0.013	0.16	0.0016
700	24.0	462	0.1321	13.46	0.264	3.78	0.0074
		6	0.0023	0.19	0.006	0.07	0.0011
725	24.0	455	0.0997	13.23	0.305	5.01	0.0081
		4	0.0013	0.11	0.006	0.07	0.0012
750	19.4	413	0.0924	11.87	0.258	5.41	0.0065
		5	0.0014	0.13	0.005	0.08	0.0013
775	18.3	396	0.0828	11.33	0.284	6.04	0.0074
		5	0.0013	0.14	0.005	0.10	0.0014
820	22.3	385	0.0657	10.95	0.367	7.60	0.0080
		4	0.0009	0.11	0.006	0.11	0.0012
875	32.4	348	0.0559	9.81	0.364	8.94	0.0071
		3	0.0007	0.07	0.004	0.11	0.0010
925	35.0	323	0.0521	9.03	0.250	9.59	0.0077
		3	0.0006	0.07	0.003	0.12	0.0010
975	42.9	292	0.0463	8.10	0.157	10.79	0.0064
		2	0.0006	0.05	0.002	0.13	0.0005
1025	36.5	281	0.0392	7.78	0.188	12.76	0.0080
		2	0.0005	0.06	0.002	0.16	0.0006
1075	21.0	312	0.0267	8.71	0.212	18.73	0.0116
		4	0.0004	0.11	0.004	0.30	0.0016
1150	17.7	316	0.0223	8.82	0.200	22.41	0.0154
		6	0.0005	0.16	0.005	0.48	0.0012
1250	6.7	370	0.0239	10.50	0.157	20.88	0.0173
		15	0.0011	0.47	0.009	0.97	0.0022
1450	6.4	580	0.0245	17.49	0.143	20.37	0.0393
		20	0.0010	0.69	0.007	0.83	0.0034
Zagami CG-Px2, 23.2 mg							
300	0.31	3783	0.2496	330.47	0.796	2.204	1.0492
		295	0.0468	61.60	0.158	0.413	0.2021
400	4.51	332	0.6517	9.36	0.159	0.844	0.0214
		10	0.0215	0.29	0.007	0.028	0.0025
475	8.25	296	0.9397	8.26	0.124	0.585	0.0127
		5	0.0205	0.16	0.004	0.013	0.0013

Table A1. (Continued). Appendix of argon isotopic data. Columns from left to right give extraction temperature, ^{39}Ar concentration in $10^{-9} \text{ cm}^3\text{STP/g}$, age in Myr, K/Ca ratio, and Ar isotopic ratios normalized to ^{39}Ar . Uncertainties are given beneath the age and all ratios.

Temp. (°C)	^{39}Ar (cc/g)	Age (Myr)	K/Ca ±	40/39 ±	38/39 ±	37/39 ±	36/39 ±
515	6.56	285	1.1064	7.93	0.121	0.497	0.0136
		6	0.0278	0.18	0.004	0.012	0.0016
550	5.07	304	1.0498	8.48	0.171	0.524	0.0099
		6	0.0265	0.19	0.006	0.013	0.0016
600	5.14	350	0.6813	9.89	0.311	0.807	0.0050
		6	0.0136	0.17	0.008	0.016	0.0011
660	4.04	771	0.2385	24.67	0.790	2.306	0.0133
		55	0.0213	2.17	0.099	0.206	0.0036
720	1.72	1832	0.0526	81.44	2.350	10.46	0.0593
		26	0.0013	1.80	0.054	0.254	0.0065
780	0.77	1988	0.0252	93.02	6.876	21.85	0.0787
		52	0.0011	4.02	0.307	0.971	0.0123
850	0.57	2283	0.0118	117.8	11.197	46.71	0.1024
		73	0.0007	6.6	0.644	2.68	0.0167
925	0.58	2751	0.00696	166.3	5.769	79.07	0.1892
		81	0.00040	9.5	0.332	4.565	0.0219
1000	0.89	2445	0.00233	133.2	2.509	236.5	0.2386
		55	0.00010	5.4	0.105	9.92	0.0190
1075	0.81	3233	0.00062	231.5	2.841	888.5	0.6767
		78	0.00003	12.0	0.149	46.9	0.0490
1135	0.34	3658	0.00016	305.2	4.480	3386.	2.1758
		227	0.00002	44.1	0.651	490.7	0.3370
1200	0.18	3233	0.00012	231.5	4.654	4431.0	2.7134
		370	0.00003	56.9	1.155	1091.	0.6938
1300	0.25	3300	0.00014	2412.	4.158	4029.0	2.5296
		314	0.00003	50.2	0.865	837.2	0.5435
1450	0.14	2592	0.00051	148.3	1.377	1079.	1.0633
		358	0.00013	38.6	0.365	281.	0.2863
Zagami FG-Px2, 23.6 mg							
300	1.35	2078	0.3276	99.9	0.469	1.68	0.3354
		73	0.0198	5.9	0.031	0.10	0.0233
430	4.29	365	0.6222	10.37	0.003	0.88	0.0346
		14	0.0266	0.43	0.002	0.04	0.0031
500	6.88	333	0.8607	9.35	0.153	0.64	0.0130
		6	0.0184	0.17	0.004	0.01	0.0015
550	6.21	313	0.9146	8.75	0.188	0.60	0.0084
		5	0.0186	0.15	0.005	0.01	0.0014
600	5.24	354	0.4597	10.02	0.347	1.20	0.0083
		6	0.0092	0.17	0.008	0.02	0.0015
650	2.82	643	0.2401	19.78	0.713	2.29	0.0180
		11	0.0054	0.39	0.018	0.05	0.0029
725	2.17	1891	0.0514	85.56	2.483	10.71	0.0834
		27	0.0013	1.93	0.057	0.26	0.0060
800	0.96	2025	0.0188	95.73	7.593	29.26	0.0929
		52	0.0008	4.09	0.331	1.29	0.0116
875	0.67	2062	0.0110	98.64	7.321	49.99	0.1263
		70	0.0006	5.62	0.425	2.89	0.0167
950	0.82	1905	0.0063	86.61	2.466	87.18	0.1372
		54	0.0003	3.93	0.116	4.06	0.0150

Table A1. (*Continued*). Appendix of argon isotopic data. Columns from left to right give extraction temperature, ^{39}Ar concentration in $10^{-9} \text{ cm}^3\text{STP/g}$, age in Myr, K/Ca ratio, and Ar isotopic ratios normalized to ^{39}Ar . Uncertainties are given beneath the age and all ratios.

Temp. (°C)	^{39}Ar (cc/g)	Age (Myr)	K/Ca ±	40/39 ±	38/39 ±	37/39 ±	36/39 ±
1025	0.85	2100	0.0016	101.8	2.089	346.2	0.2723
		55	0.0001	4.4	0.095	15.51	0.0225
1100	0.63	3293	0.0004	240.45	3.250	1416.	0.9193
		100	0.0000	15.77	0.215	93.9	0.0796
1175	0.33	3454	0.0001	267.1	5.267	5618.	3.1134
		264	0.0000	45.7	0.907	964.	0.5687
1275	0.22	3089	0.0001	209.7	4.485	4799.	2.7426
		331	0.0000	46.9	1.013	1076.	0.6435
1450	0.11	2564	0.0006	145.2	1.084	891.4	0.9669
		375	0.0002	39.8	0.323	244.6	0.2959
Zagami FG-Px1, 20.0 mg							
300	0.20	6337	0.1427	1500.	2.826	3.853	4.8575
		321	0.0263	275.	0.530	0.711	0.8975
400	2.35	635	0.3442	19.45	0.371	1.598	0.0787
		35	0.0230	1.28	0.027	0.107	0.0080
475	3.99	666	0.4169	20.60	0.291	1.319	0.0850
		30	0.0226	1.09	0.017	0.071	0.0061
525	5.12	439	0.6336	12.71	0.164	0.868	0.0380
		15	0.0258	0.50	0.008	0.035	0.0032
570	5.77	351	0.7132	9.90	0.157	0.771	0.0159
		8	0.0182	0.23	0.006	0.020	0.0020
625	6.09	390	0.5238	11.14	0.230	1.050	0.0092
		6	0.0100	0.18	0.006	0.020	0.0015
700	5.96	1000	0.1355	34.18	0.542	4.057	0.0274
		37	0.0066	1.63	0.036	0.199	0.0046
765	3.58	1863	0.0561	83.43	1.329	9.804	0.0502
		17	0.0009	1.15	0.020	0.167	0.0040
825	1.88	1779	0.0347	77.53	2.107	15.85	0.0584
		30	0.00100	1.98	0.056	0.436	0.0067
900	1.83	1694	0.02245	71.83	1.987	24.49	0.0654
		27	0.00058	1.70	0.050	0.631	0.0071
975	1.74	1509	0.00783	60.31	1.167	70.22	0.0905
		26	0.00021	1.48	0.032	1.866	0.0085
1050	1.42	2183	0.00154	108.5	1.449	356.4	0.2645
		39	0.00005	3.3	0.046	11.26	0.0180
1125	1.05	2954	0.00038	191.0	1.978	1453.	0.8759
		75	0.00002	9.8	0.104	75.9	0.0677
1200	0.38	2996	0.00010	196.6	5.170	5441.	2.9183
		256	0.00002	34.4	0.911	954.	0.5465
1300	0.30	3226	0.00012	229.6	3.993	4447.	2.4841
		283	0.00002	43.2	0.758	837.	0.4968
1450	0.08	3171	0.00047	221.3	1.335	1160.	1.3692
		545	0.00017	80.7	0.496	423.	0.5114